Available online at www.sciencedirect.com

ScienceDirect

Physics Letters B 662 (2008) 417–423

PHYSICS LETTERS B

www.elsevier.com/locate/physletb

Unitarisation and black-disk limit at the LHC in the presence of a hard pomeron

J.-R. Cudell [a,*], O.V. Selyugin [b]

[a] *Institut de Physique, Bât. B5a, Université de Liège, Sart Tilman, B4000 Liège, Belgium*

[b] *Bogoliubov Laboratory of Theoretical Physics, JINR, 141980 Dubna, Moscow Region, Russia*

Received 6 December 2006; received in revised form 13 March 2008; accepted 15 March 2008

Available online 20 March 2008

Editor: A. Ringwald

Abstract

Recent models of soft diffraction include a hard pomeron pole besides the usual soft term. Such models violate the black-disk limit around Tevatron energies, so that they need to be supplemented by a unitarisation scheme. Two standard schemes are considered in this Letter, and we show that they lead to an uncertainty at the LHC much larger than previously estimated. We also examine the signature of unitarisation on various small-t observables, the slope in t of the elastic cross section, or the ratio of the real to imaginary parts of the scattering amplitude, and show that the existence of a unitarised hard pomeron in soft scattering may be confirmed by LHC data.

PACS: 13.85.Lg; 13.85.-t; 13.85.Dz; 12.40.Nn; 11.80.Fv

Keywords: Saturation; Unitarisation; Hard pomeron

0. Introduction: Hard poles

Experimental data reveal that total cross sections grow with energy. This means that the leading contribution in the high-energy limit is given by the rightmost singularities in the complex-j plane, the pomerons, with intercepts exceeding unity. In the framework of perturbative QCD, the leading singularity is expected to exceed unity by an amount proportional to α_s [1]. At leading-log, one obtains a leading singularity at $J - 1 = 12\alpha_S \log 2/\pi$.

Donnachie and Landshoff have shown that DIS and quasi-elastic vector-meson production data at HERA could be well reproduced if one included both a soft pomeron, and a hard pomeron with an intercept of the order of 1.4 [2]. They also showed that their parametrisation could be made consistent with DGLAP evolution [3], both at small and high x. From this, they were able to extract parton distribution functions [4]. So their works imply that there is a non-negligible hard pomeron component at large Q^2 and for large masses.

However, from analytic S-matrix theory, it is expected that the singularities of the exchanges do not depend on the external kinematics. Hence, although perturbative calculations can be justified only for the scattering of far off-shell particles, and although the hard pomeron seems to be present only at short distances, a trace of it should be present at long distance.

In a recent study [5], we have indeed found that forward data (total cross sections and the ratios of the real part to the imaginary part of the amplitude) could be fitted well by a combination of a soft pomeron (which would be purely non-perturbative) and a hard pomeron. The expression of the leading terms of the total cross sections for the scattering of a on p becomes

$$\sigma_{\rm tot}^{ap} = \frac{1}{2P\sqrt{s}}\,\Im\mathrm{m}\,A(s,t=0), \tag{1}$$

where A is the hadronic amplitude

$$\Im\mathrm{m}\,A(s,t=0) \approx H_a\left(\frac{s-u}{2s_1}\right)^{\alpha_H(0)} + S_a\left(\frac{s-u}{2s_1}\right)^{\alpha_S(0)} \tag{2}$$

* Corresponding author.
E-mail addresses: j.r.cudell@ulg.ac.be (J.-R. Cudell), selugin@theor.jinr.ru (O.V. Selyugin).

0370-2693
doi:10.1016/j.physletb.2008.03.033

Table 1
Parameters of the leading singularities of the fits of Ref. [5] for $\sqrt{s}$ from 5 to 100 GeV

Parameter	Value	Error	Parameter	Value	Error
$\alpha_S(0)$	1.0728	0.0008	$\alpha_H(0)$	1.45	0.01
S_p	56.2	0.3	H_p	0.10	0.02
S_π	32.7	0.2	H_π	0.28	0.03
S_K	28.3	0.2	H_K	0.30	0.03
S_γ	0.174	0.002	H_γ	0.0006	0.0002

and where P is the beam momentum in the target frame, s, t and u are the Mandelstam variables, $s_1 = 1$ GeV^2, and the parameters are given in Table 1. We insist that throughout this Letter the latter will be kept fixed. The inclusion of these two pomerons, together with the use of integral dispersion relations, and the addition of subleading meson trajectories (ρ/ω and a/f), leads to a successful description of all pp, $\bar{p}p$, $\pi^\pm p$, $K^\pm p$, γp and $\gamma\gamma$ data for $\sqrt{s} \leqslant 100$ GeV. We must stress here that the χ^2 of the fit is as good as that of the best parametrisations to the data considered in [6,7]. It is also the only model that can naturally describe both soft hadronic cross section and HERA DIS and vector-meson quasielastic production data.

The fit can be extended to higher energies, but the hard pomeron then decouples from the proton. The problem is that the fast-growing hard pomeron leads to a violation of unitarity (an elastic cross section bigger than the total cross section) for values of s smaller than 1 TeV. In [5], we used a simple ansatz to unitarise the hard pole. However, we did not examine the uncertainties linked to it, as we simply wanted to show that it was possible to extend the fit to higher energies. In this Letter, we pursue two goals: first of all, we give an estimate of the value of the total cross section at the LHC in the presence of a hard pomeron. Secondly, we propose several signatures of unitarisation which would in principle allow to decide which type of scheme is correct, and to confirm the presence of hard-pomeron exchanges.

Section 1 will be devoted to a reminder of unitarisation, and of the impact-parameter ($\vec{b}$) formalism. Section 2 will consider the "minimal" unitarisation, which cuts off the amplitude in impact parameter once it saturates the black-disk limit—we shall refer to this scheme as the saturation scheme. Section 3 will consider analytic unitarisation schemes. Finally, putting everything together, we shall show that the cross section at the LHC should be large, of the order of 150 mb. We shall explain what some generic consequences of unitarisation will be for observables at the LHC.

1. Unitarity and black-disk limit

The simplest expression of the unitarity constraints can be obtained from partial-wave amplitudes. We can write

$$A(s,t) = 8\pi \sum_l (2l+1)\mathcal{F}_l(s) P_l(\cos\theta_s). \tag{3}$$

At high energy and small angle, one can rewrite $l \approx \frac{b\sqrt{s}}{2}$, so that the partial-wave decomposition can be rewritten in impact-parameter space as

$$A\big(s, t=-q^2\big) = 2s \int d^2\vec{b}\, e^{-i\vec{q}.\vec{b}} \mathcal{F}(s,b). \tag{4}$$

In terms of $\mathcal{F}(s,b) = \int d^2\vec{q}\, e^{i\vec{q}.\vec{b}} A(s,t)/(8\pi^2 s)$, the total and elastic cross sections are given by

$$\sigma_{\rm tot} = 4\pi \int b\, db\, \Im{\rm m}\, \mathcal{F}(s,b) \tag{5}$$

and

$$\sigma_{\rm el} = 2\pi \int b\, db \left|\mathcal{F}(s,b)\right|^2. \tag{6}$$

One can then show that unitarity of the S matrix, $SS^\dagger = 1$, together with analyticity, and with the normalisation used in (5) and (6), requires that

$$0 \leqslant \left|\mathcal{F}(s,b)\right|^2 \leqslant 2\,\Im{\rm m}\, \mathcal{F}(s,b) \leqslant 4. \tag{7}$$

At high energies, as $\Im{\rm m}\,\mathcal{F} \propto s^\Delta$ with $\Delta > 0$, the scattering amplitude $\mathcal{F}(s,b)$ reaches the unitarity bound for some value $b_u(s)$ of the impact parameter.

However, before this happens, another regime is reached, which we shall call the saturation regime, and where the inelasticity $2\,\Im{\rm m}\,\mathcal{F}(s,b) - |\mathcal{F}(s,b)|^2$ reaches its maximum, i.e. if

$$\Im{\rm m}\, \mathcal{F}(s,b) = 1. \tag{8}$$

This is the region where the proton becomes partially black, and it is usually referred to as the black-disk limit. The imaginary part of $\mathcal{F}$ is usually noted as $\Gamma(s,b)$ and called the profile function. $\Gamma(s,b) = 1$ at some distance $b_S(s)$ between scattering particles means that the inelastic amplitude has reached its maximum value.

What happens then is largely unclear. There is no unique procedure to unitarise. In the following, we shall consider two main schemes: the minimal one, where unitarisation freezes the profile function at 1: this is the minimum possibility for the restoration of unitarity, as it does not affect in any way the low-energy data. We shall refer to it as "saturation of the profile function". We shall also consider the predictions of a simple eikonal scheme, in which multiple exchanges prevent the profile function from reaching 1. We shall refer to this kind of scheme as "analytic unitarisation".

2. Saturation

If we take a single simple pole for the scattering amplitude,[1] with an exponential form factor of slope d,

$$A(s,t) = S_p s^{\alpha_S(0)+\alpha' t} e^{dt}, \tag{9}$$

then the radius of saturation and its dependence on energy can be obtained analytically:

$$b_S(s)^2 = 4(d+\alpha'\log s)\log\left(\frac{S_p s^{\alpha_S(0)-1}}{2(d+\alpha'\log s)}\right). \tag{10}$$

[1] As we shall consider energies ranging from 100 GeV to 14 TeV, we shall approximate $\frac{s-u}{2} \approx s$ in the following.

Table 2
Parameters of the elastic pomeron form factor, see Eq. (12)

Parameter	Value	Parameter	Value (GeV^{-2})
h_1	0.55	d_1	5.5
h_2	0.25	d_2	4.1
h_3	0.20	d_3	1.2

Approximating $\sigma_{\rm tot} \approx 2\pi b_S^2(s)$, one sees that the total cross section grows logarithmically at medium energies and like $\log^2 s$ at very high energies.

In our model [5,8], the pp elastic scattering amplitude is proportional to the hadrons form-factors and can be approximated at small t as:

$$A(s,t) = \big[H_p F_H(t)(s/s_1)^{\alpha_H(0)} e^{\alpha'_H t \log(s/s_1)} + S_p F_S(t)(s/s_1)^{\alpha_S(0)} e^{\alpha'_S t \log(s/s_1)}\big], \quad (11)$$

where the couplings and intercepts are given in Table 1. The study of Ref. [8] of small-t elastic scattering shows that the slope α'_S of the soft pomeron trajectory is slightly higher than its classical value [9,10], and we shall take $\alpha'_S = 0.3$ GeV^2. The slope of the hard pomeron trajectory is evaluated [2,8] to be $\alpha'_H = 0.1$ GeV^2. The normalisation $s_1 = 1$ GeV^2 will be dropped below and s also contains implicitly the phase factor $\exp(-i\pi/2)$, corresponding to crossing symmetry.

A small-t analysis [8] indicates that the form factor $F_S(t)$ is close to the square of the Dirac elastic form factor, and can be approximated by the sum of three exponentials with fixed parameters [10]:

$$F_S(t) = \left(\frac{4m_p^2 - 2.79t}{4m_p^2 - t}\frac{1}{1 - t/\Lambda^2}\right)^2 \approx h_1 e^{d_1 t} + h_2 e^{d_2 t} + h_3 e^{d_3 t}, \quad (12)$$

where m_p is the mass of the proton, $\Lambda^2 = 0.71$ GeV^2. The other parameters are given in Table 2. For the hard pomeron, the form factor is rather uncertain [8], and we assume that it can be taken equal to $F_S(t)$.

We then obtain in the impact parameter representation a specific form for the amplitude in $\vec{b}$ space, $\mathcal{F}_0(s,b)$ [11], which we show in Fig. 1:

$$\mathcal{F}_0(s,b) = \frac{S_p}{s}\sum_i \frac{2h_i}{r_{i,S}} s^{\alpha_S(0)} \exp\big(-b^2/r_{i,S}^2\big) + (S \to H)$$

with

$$r_{i,S}^2 = 4\big(d_i + \alpha'_S \log(s)\big), \quad (13)$$

$$r_{i,H}^2 = 4\big(d_i + \alpha'_H \log(s)\big). \quad (14)$$

One can see that at some energy and at small b,

$$\Gamma_0(s,b) = \Im\mathrm{m}\,\mathcal{F}_0(s,b) \quad (15)$$

reaches the black disk limit. For our model, this will be in the region $\sqrt{s} \approx 1.5$ TeV.

Saturation will then control the behaviour of $\sigma_{\rm tot}$ at higher energies. We assume that once it reaches i, the amplitude does not change anymore and remains equal to i: recombination must be maximal for black protons. But this freezing of the profile function must be implemented carefully, and we have to introduce 3 parameters to describe it: one cannot simply cut the profile function sharply as this would lead to a non-analytic amplitude, and to specific diffractive patterns in the total cross section and in the slope of the differential cross sections. Furthermore, we have to match at large impact parameter the behaviour of the unsaturated profile function.

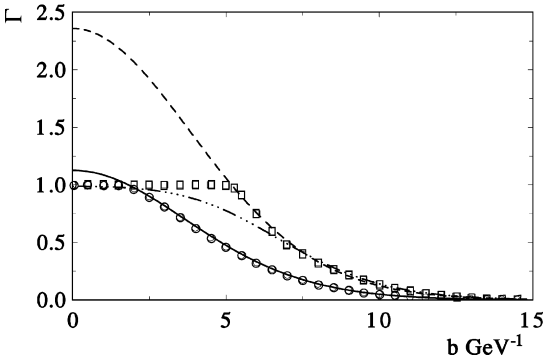

Fig. 1. The profile function for proton–proton scattering: at $\sqrt{s} = 2$ TeV without (Eq. (15)) and with (Eq. (16)) saturation (hard line and circles), at $\sqrt{s} = 14$ TeV without and with saturation (the dashed line and squares), or from the eikonal scheme (Eq. (26)) (dash-dotted line).

We use an analytic interpolating function, which is equal to 1 for large impact parameters and which forces the profile function to approach 1 at the saturation scale b_S as a Gaussian. Analyticity of the function enables us to use a complex s as before to obtain the real part.

We assume saturation starts at a point b_0 a little before b_S, and that the profile function is 1 for $b < b_0$. The saturated profile, $\Gamma_s(s,b)$, is otherwise given by

$$\Gamma_s(s,b) = \frac{\Gamma_0(s, b - \frac{b_0}{1+((b-b_0)/b_z)^2})}{1 + (\Gamma_0(s,0) - 1)\exp[-(\frac{(b-b_0)}{b_y(s)})^2]}. \quad (16)$$

We find that we need to assume that the scale in the Gaussian is s-dependent because the slope of the profile function decreases with energy. A reasonable match is provided by $b_y = 32/\log s$, which is about 5 GeV^{-1} at the Tevatron. We shall give our results for $b_z^2 = 2$ GeV^{-2} and $b_0/b_s = 97.5\%$.

We show in Fig. 2 the behaviour of the total cross section at high energies. We see that saturation brings in a significant decrease of the LHC cross section. However, it is also clear that the simple saturation considered here is not enough, as the total cross section at the Tevatron will be 85 mb, which is 2 standard deviations from the CDF result.

Nevertheless, the contribution of the hard pomeron has been fixed by looking at low-energy data. There, its contribution is small, and one can still get a good fit by varying the intercept and the coupling. Thus we show in Fig. 3 the effect of changing one or the other. We see that if saturation is the driving mechanism, then the coupling would need to be reduced[2] to 0.06

[2] Note that Ref. [12] also predicted a large LHC cross section, but did not use a unitarisation scheme, and instead used a very small hard pomeron coupling, about 4 times smaller than considered here.

or the intercept to 1.41 in order to accommodate the Tevatron point in this scheme. This would lead to an LHC cross section slightly larger than 130 mb. As we want to show qualitatively what the effect of saturation might be, we keep the parameters of Table 1 in the following.

The saturation regime will have some major effects at the LHC. We show in Fig. 4 that the elastic cross section will be somewhat affected, and that its growth will be tamed: the ratio $\sigma_{\rm el}/\sigma_{\rm tot}$ will start a slow growth towards 0.5. But more importantly, the small-t data will look quite different. We show in Fig. 5 the behaviour of the ratio of the real-to-imaginary part of the cross section, both in the bare and in the saturated case. From it, we see that the small-t slope of ρ will be one of the most striking features of saturation. If this is not measurable at the LHC, then one can also consider the slope of the differential elastic cross section, which we show in Fig. 6. We see that saturation increases the slope at small $|t|$, and predicts a fast drop around $|t| = 0.25$ GeV^2, when one enters the region of the dip.

In fact, saturation naturally predicts a small increase of the slope with t at small $|t|$. To understand this, let us take the simple form of the black disk with a sharp edge at radius $R \sim b_S(s)$ of Eq. (10), or Fig. 1. The scattering amplitude can then be represented as

$$A(s, t = 0) \sim \frac{J_1(\sqrt{-t}R)}{\sqrt{-t}R}.$$

In this case, the slope of the differential cross section at small momentum transfer will be

$$B_{\rm BDL} \sim R^2/4 + R^4/32|t|. \tag{17}$$

Hence the slope will grow with increasing $|t|$ at small momentum transfer, as can be seen in Fig. 6.

This strong dependence of the slope and of ρ on t imply that it may be necessary to measure both of them to obtain a reliable measurement of the total cross section [13].

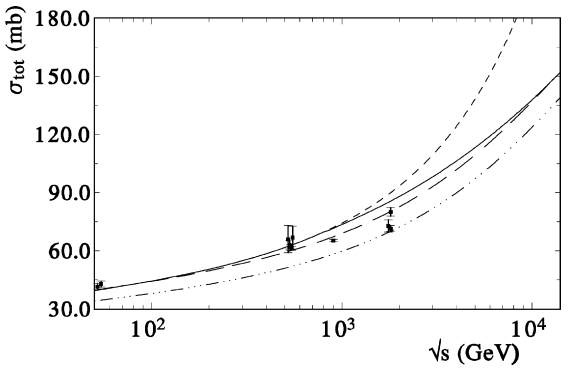

Fig. 2. The total cross section as a function of $\sqrt{s}$, for the bare amplitude (short dashes), the saturated amplitude (plain curve), the eikonalised amplitude (dash-dot-dot), and for a renormalised eikonal (long dashes).

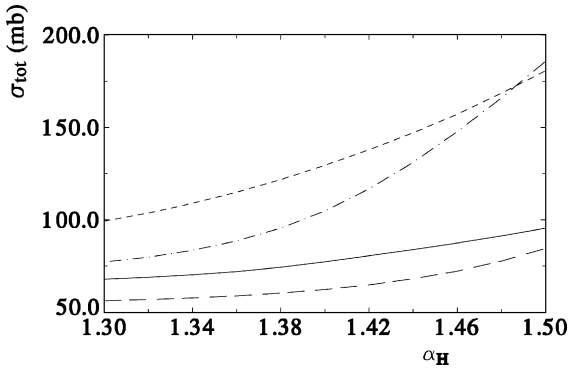

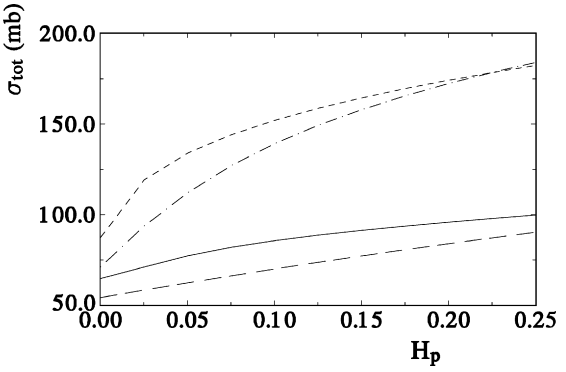

Fig. 3. The total cross section at the Tevatron (lower curves) and at the LHC (upper curves) as a function of the intercept (left) and of the coupling (right) of the hard pomeron for a saturated amplitude (plain curves and short dashes) and for an eikonalised amplitude (long dashes and dash-dots).

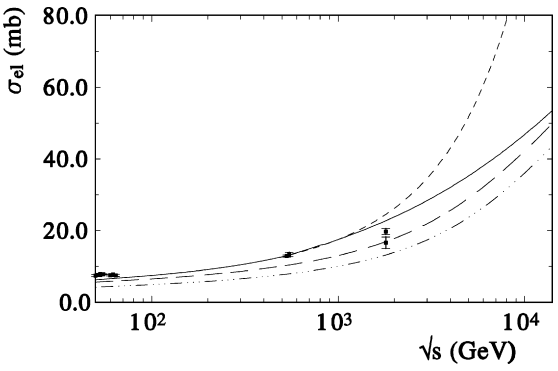

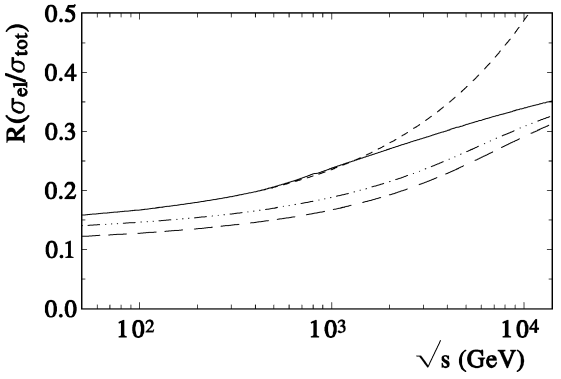

Fig. 4. The elastic cross section as a function of s (left), and its ratio to the total cross section (right), for the bare amplitude (short dashes), the saturated amplitude (plain curve), the eikonalised amplitude (dash-dot-dot), and for a renormalised eikonal (long dashes).

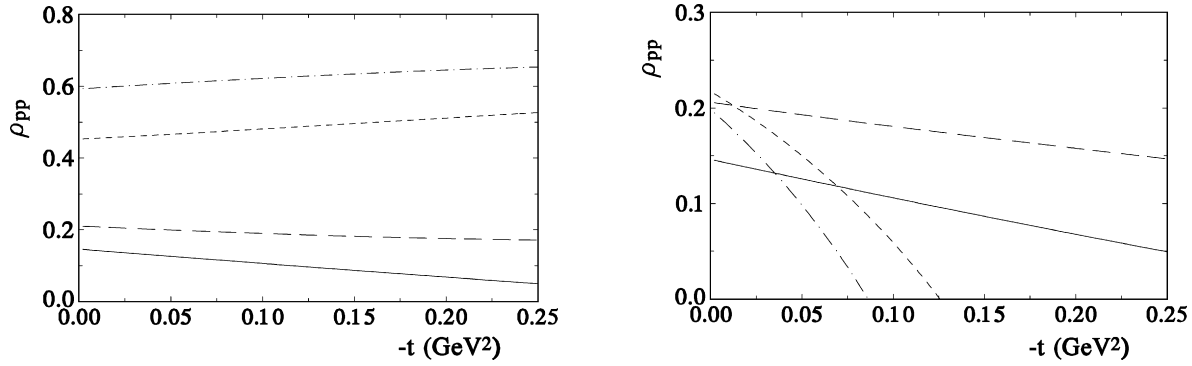

Fig. 5. The ratio of the real to the imaginary part of the amplitude as a function of t, for the bare (left figure) and the saturated (right figure) amplitudes at various energies: 100 GeV (plain curve), 500 GeV (long dashes), 5 TeV (short dashes) and 14 TeV (dash-dotted curve).

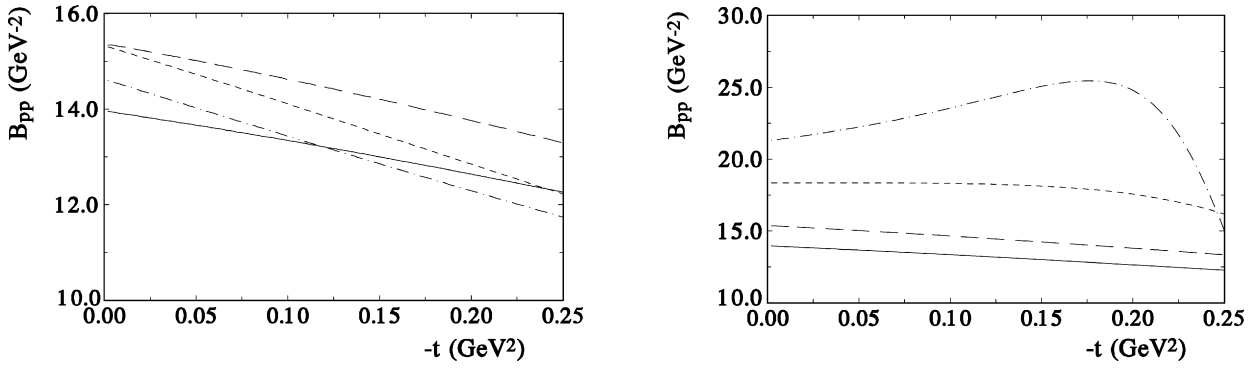

Fig. 6. The slope of the elastic differential cross section as a function of t, for the bare (left figure) and saturated (right figure) amplitudes at various energies: 100 GeV (plain curve), 500 GeV (long dashes), 5 TeV (short dashes) and 14 TeV (dash-dotted curve).

3. Analytic unitarisation schemes

As we have seen, in $\vec{b}$ space, unitarisation can be written

$$2\,\Im\mathrm{m}\,\mathcal{F} - (\Im\mathrm{m}\,\mathcal{F})^2 - (\Re\mathrm{e}\,\mathcal{F})^2 = g_{\rm in} > 0. \tag{18}$$

The general solution can be obtained iff $g_{\rm in} < 1$, and can be written $\mathcal{F} = i(1-(1-g_{\rm in})e^{i\Phi})$. We can rewrite it using the opacity Ω so that $(1-g_{\rm in}) = e^{-\Omega}$

$$\mathcal{F} = i\big(1-e^{-\Omega+i\Phi}\big) = i\big(1-e^{i\chi(s,b)}\big). \tag{19}$$

Any unitarisation method has to lead to such a form for the amplitude. The ambiguity however comes when one tries to identify $g_{\rm in}$ and Φ in formula (19) with the physics input. It is known from potential models that in non-relativistic physics one can think of the Taylor expansion of (19) as a description of successive interactions with the potential. Here, however, we have no potential, so that the identification of each term with successive pomeron exchanges is not obvious.

The usual approach is to assume that the Taylor expansion of (19) is such that the nth term corresponds to n-pomeron exchange. In this case, we take the eikonal form for the scattering amplitude.

$$A_e(s,t=0) = 2s\int d^2b\big[1-\exp\big(i\mathcal{F}_0(s,b)\big)\big].$$

Before giving the results in this approach, a few comments are in order. First of all, the eikonal is only a model. Indeed, it is known [14] that it does not reproduce properly the s-channel cuts of the scattering amplitude coming from multiple exchanges. For instance, already the second term, corresponding to the two-pomeron cut, could have a suppression due to the structure of the proton [10].

The eikonal scheme however produces results which are similar to those of saturation, so that it makes sense to compare these two schemes. Indeed, we take the eikonal in factorised form

$$\chi(s,b) = h(s)\,f(b), \tag{20}$$

with $h(s) = s^{\Delta}$, and assume simple functional forms for the form factor $f(b)$, which allow an analytical treatment. If one considers a Gaussian form

$$f(b) \sim \exp\big(-b^2/R^2\big), \tag{21}$$

one obtains

$$A(s,t=0) \sim iR^2\big(\Gamma\big(0,s^{\Delta}\big) + \gamma + \Delta\log s\big), \tag{22}$$

where

$$\Gamma(a,z) = \int_z^{\infty} t^{a-1}e^{-t}\,dt$$

and, in our case,

$$\Gamma\big(0,s^{\Delta}\big) \to 0, \quad s\to\infty. \tag{23}$$

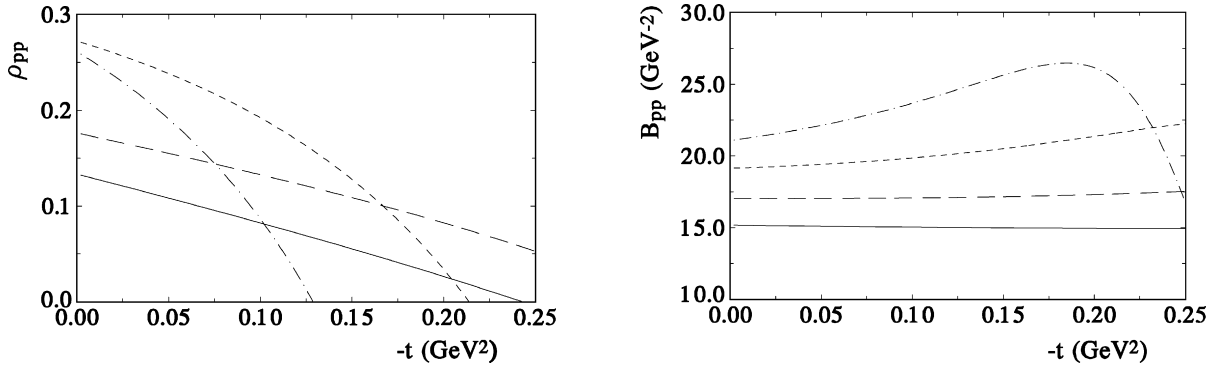

Fig. 7. The ratio of the real to the imaginary part of the amplitude (left), and the slope of the elastic differential cross section (right) as functions of t for the eikonalised amplitude at various energies: 100 GeV (plain curve), 500 GeV (long dashes), 5 TeV (short dashes) and 14 TeV (dash-dotted curve).

If R^2 is independent from s, we have

$$\sigma_{\rm tot} \sim \log(s), \tag{24}$$

whereas for R^2 growing like $\log(s)$, we obtain

$$\sigma_{\rm tot} \sim \log^2(s), \tag{25}$$

so the total cross section respects the Froissart bound.[3]

Hence we can now see whether the saturation effects that we found in the previous section depend on the picture of saturation, or depend only on the onset of unitarising cuts.

We show in Fig. 1 that, in this case, the profile function

$$\Gamma_e(s,b) = \Im\mathrm{m}\big[1 - \exp\big(i\mathcal{F}_0(s,b)\big)\big] \tag{26}$$

never saturates: the cuts actually reduce the cross section from the start, and never allow $\Gamma_e(s,b)$ to become larger than 1. This means, as is shown in Fig. 2 that eikonalisation will give a suppression, even at lower energies. So one needs to modify slightly the parameters of Table 1, to recover the low-energy fit. We find that multiplying the couplings by 1.2 provides such an agreement, and refer to this as the "renormalised eikonal", shown in Fig. 2. We see that both curves are very close at the LHC, but exceed considerably previous estimates [16]: whereas the total cross section at the LHC was predicted to be $111.5 \pm 1.2^{+4.1}_{-2.1}$ mb, it is now 152 mb.

In a similar manner, Fig. 4 shows that the elastic cross section also gets large corrections from the cuts at lower energies. Again, the renormalised eikonal is close to the saturated curve at low energy, but this time deviates at higher energies, so that the ratio of the elastic cross section to the total cross section changes by about 10%.

We had seen that a striking feature of saturation was the behaviour of the real part of the amplitude at small-t, as the ρ parameter would have a drastic change of slope. We find that such an effect will also be present in the eikonal case (see Fig. 7), although the real part will be much bigger in this case. Similarly, we also show in Fig. 7 the behaviour of the slope of the differential elastic cross section. Again, we see that it increases at small-t, and then decreases towards the dip.

4. Conclusion

Now the structure of the diffractive scattering amplitude cannot be obtained from first principles or from QCD. The procedure used to extract such structure and parameters of the elastic scattering amplitude from the experimental data requires some different assumptions. If we assume that the hard pomeron is present in soft data, it will lead to a cross section of the order of 150 mb (a similar conclusion, via a different argument, has been reached in [12]).[4] The uncertainty in this number is quite large, as unitarisation and saturation schemes are numerous. Hence it seems that the total cross section can be anywhere between 108 mb [16] and 150 mb.

Other observables may be used to decide whether one has a simple extrapolation of the lower-energy data, such as in [16], or one is entering a new regime of unitarisation. Indeed, in the presence of the hard pomeron, the saturation effects, which must then be present at LHC energies, can change the behaviour of the real part of the cross section making it smaller than expected, especially in the near-forward region, and of the slope of the differential elastic scattering cross section.

Despite the lack of an absolute prediction for total cross sections, the observation of such features would be a clear sign that a new regime of strong interactions has been reached.

Acknowledgements

O.V.S. acknowledges the support of FNRS (Belgium) for visits to the University of Liège where part of this work was done. We thank E. Martynov, S. Lengyel, G. Soyez and P.V. Landshoff for discussions.

References

[1] L.N. Lipatov, Sov. J. Nucl. Phys. 23 (1976) 338;
E.A. Kuraev, L.N. Lipatov, V.S. Fadin, Sov. Phys. JETP 45 (1977) 199;

[3] The eikonal does not always guarantee unitarisation. Although it obeys Eq. (7) for all values of b, it can produce, after integration, amplitudes that violate the Froissart bound depending on the b dependence of the form factor [15]. The form factors that we use lead to a cross section that does respect the Froissart bound.

[4] This does not contradict the cosmic-ray data as the uncertainties in deconvoluting the p-air inelastic cross section to obtain the total cross section are large and depend on the unitarisation scheme chosen [17].

I.I. Balitsky, L.N. Lipatov, Sov. J. Nucl. Phys. 28 (1978) 822.
[2] A. Donnachie, P.V. Landshoff, Phys. Lett. B 437 (1998) 408, hep-ph/9806344;
A. Donnachie, P.V. Landshoff, Phys. Lett. B 478 (2000) 146, hep-ph/9912312.
[3] J.R. Cudell, A. Donnachie, P.V. Landshoff, Phys. Lett. B 448 (1999) 281, hep-ph/9901222;
J.R. Cudell, A. Donnachie, P.V. Landshoff, Phys. Lett. B 526 (2002) 413, Erratum;
A. Donnachie, P.V. Landshoff, Phys. Lett. B 533 (2002) 277, hep-ph/0111427.
[4] A. Donnachie, P.V. Landshoff, Phys. Lett. B 550 (2002) 160, hep-ph/0204165.
[5] J.R. Cudell, E. Martynov, O.V. Selyugin, A. Lengyel, Phys. Lett. B 587 (2004) 78, hep-ph/0310198;
J.R. Cudell, E. Martynov, O.V. Selyugin, A. Lengyel, Nucl. Phys. B (Proc. Suppl.) 152 (2006) 79, hep-ph/0408332.
[6] J.R. Cudell, et al., Phys. Rev. D 65 (2002) 074024, hep-ph/0107219.
[7] W.M. Yao, et al., Particle Data Group, J. Phys. G 33 (2006) 1.
[8] J.R. Cudell, A. Lengyel, E. Martynov, Phys. Rev. D 73 (2006) 034008, hep-ph/0511073.
[9] A. Donnachie, P.V. Landshoff, Nucl. Phys. B 231 (1984) 189.
[10] A. Donnachie, G. Dosch, O. Nachtmann, P.V. Landshoff, Pomeron physics and QCD, in: Camb. Monogr. Part. Phys. Nucl. Phys. Cosmol., vol. 19, 2002, p. 1.
[11] J.R. Cudell, O.V. Selyugin, Czech. J. Phys. 54 (2004) A441, hep-ph/0309194.
[12] P.V. Landshoff, Talk given at 11th International Conference on Elastic and Diffractive Scattering: Towards High Energy Frontiers: The 20th Anniversary of the Blois Workshops, Chateau de Blois, Blois, France, 15–20 May 2005, hep-ph/0509240.
[13] O.V. Selyugin, J.R. Cudell, arXiv: 0709.0100 [hep-ph], in: J. Bartels, K. Borras, M. Diehl, H. Jung (Eds.), Proceedings of the 12th International Conference on Elastic and Diffractive Scattering (Blois Workshop)—Forward Physics and QCD, DESY, Hamburg, 2007, p. 279, arXiv: 0712.3633 [hep-ph].
[14] P.V. Landshoff, J.C. Polkinghorne, Phys. Rev. 181 (1969) 1989.
[15] A. Kovner, U.A. Wiedemann, Phys. Rev. D 66 (2002) 051502, hep-ph/0112140.
[16] J.R. Cudell, et al., COMPETE Collaboration, Phys. Rev. Lett. 89 (2002) 201801, hep-ph/0206172.
[17] N.N. Nikolaev, Phys. Rev. D 48 (1993) 1904, hep-ph/9304283.